BIOLOGY OF REPRODUCTION (2015) **93**(2):48, 1–12
Published online before print 1 July 2015.
DOI 10.1095/biolreprod.115.130344

Mobilization of Dormant *Cnot7* mRNA Promotes Deadenylation of Maternal Transcripts During Mouse Oocyte Maturation[1]

Jun Ma, Yusuke Fukuda,[3] and Richard M. Schultz[2]

Department of Biology, University of Pennsylvania, Philadelphia, Pennsylvania

ABSTRACT

Maternal mRNAs in oocytes are remarkably stable. In mouse, oocyte maturation triggers a transition from mRNA stability to instability. This transition is a critical event in the oocyte-to-embryo transition in which a differentiated oocyte loses its identity as it is transformed into totipotent blastomeres. We previously demonstrated that phosphorylation of MSY2, an RNA-binding protein, and mobilization of mRNAs encoding the DCP1A-DCP2 decapping complex contribute to maternal mRNA destruction during meiotic maturation. We report here that *Cnot7, Cnot6l,* and *Pan2*, key components of deadenylation machinery, are also dormant maternal mRNAs that are recruited during oocyte maturation. Inhibiting the maturation-associated increase in CNOT7 (or CNOT6L) using a small interference RNA approach inhibits mRNA deadenylation, whereas inhibiting the increase in PAN2 has little effect. Reciprocally, expressing CNOT7 (or CNOT6L) in oocytes prevented from resuming meiosis initiates deadenylation of mRNAs. These effects on deadenylation are also observed when the total amount of poly (A) is quantified. Last, inhibiting the increase in CNOT7 protein results in an ~70% decrease in transcription in 2-cell embryos.

CNOT6L, CNOT7, deadenylase, early development, gamete biology, mRNA degradation, maternal recruited mRNA, oocyte maturation, PAN2

INTRODUCTION

During mouse oocyte growth, which takes about ~18 days to generate a full-grown oocyte, mRNAs are remarkably stable with a half-life of ~10–14 days [1, 2]. This stability likely reflects a strategy to accumulate mRNAs because oocyte growth, which encompasses an ~200-fold increase in volume, occurs in the absence of cell division. In addition, transcription starts to decrease starting around midgrowth such that full-grown oocytes are transcriptionally quiescent [3], which may also serve as an additional selective pressure for mRNA stability. MSY2, a germ cell-specific RNA-binding protein, is involved in global mRNA stability in mouse oocytes [4–6]. Oocytes deficient in MSY2 have about 25% less total mRNA and an injected reporter mRNA is less stable when compared to wild-type oocytes.

Oocyte maturation triggers a transition from mRNA stability to instability that culminates in degradation of thousands of different mRNAs [7, 8]. A functional eukaryotic mRNA is 5′-capped and 3′-polyadenylated, posttranscriptional modifications that control translation and mRNA stability [9]. In somatic cells, mRNA degradation is initiated by shortening or removal of the poly (A) tail by deadenylases, namely, PAN2 (catalytic component of the PAN2-PAN3 complex), CNOT6/CNOT6L/CNOT7/CNOT8 (catalytic components of the CCR4-NOT complex), or PARN [10]; PAN2-PAN3 and CCR4-NOT complexes are likely the major eukaryotic deadenylases and conserved across species [11]. Degradation from the 3′ end is triggered by sequential PAN2/PAN3- and CCR4-NOT-mediated deadenylation [12] that prepares the targeted mRNA for further degradation by the exosome complex [13]. Deadenylation triggers decapping by the DCP1A-DCP2 complex [14], which is followed by XRN1-mediated 5′-3′ exonuclease degradation [15]. Deadenylation is often the first and rate-limiting step of mRNA degradation, and once degradation initiates, the mRNA is rapidly and totally degraded, typically within minutes. In fact, turnover is so rapid that the lack of detectable intermediates has precluded a complete analysis of the degradation pathway [16]. The 5′-3′ decay appears to be the major pathway for mRNA destruction in mammalian cells [17] with 5′-3′ decay ensuring that the last translocating ribosome completes translation to yield a full-length protein product [18].

CDK-1-mediated phosphorylation of MSY2 plays a pivotal role in the transition from mRNA stability to instability [4]; phosphorylation of MSY2 appears to make endogenous mRNAs more susceptible to the RNA degradation machinery. Maturation also triggers recruitment of dormant maternal mRNAs that encode DCP1A and DCP2, and inhibiting the maturation-associated increase in DCP1A/DCP2 reduces the extent of normal degradation of mRNAs during oocyte maturation [19]. Because mRNA degradation also entails degradation from the 3′ direction, we explored the possibility that critical components of the 3′ degradation machinery are also encoded by dormant maternal mRNAs and that their recruitment during maturation contributes to mRNA degradation.

We report that CNOT7 and PAN2 are encoded by dormant maternal mRNAs and that recruitment of *Cnot7* mRNA, but not *Pan2* mRNA, is critical for deadenylation of maternal mRNAs. In addition, deadenylation of maternal mRNAs appears critical for genome activation because inhibiting the maturation-associated increase in CNOT7 inhibits transcription by ~70% in 2-cell embryos.

[1]Supported by a grant from National Institutes of Health (HD022681) to R.M.S.
[2]Correspondence: Richard Schultz, Department of Biology, University of Pennsylvania, 433 South University Avenue, Philadelphia, PA 19104. E-mail: rschultz@sas.upenn.edu
[3]Current address: Department of Obstetrics and Gynecology Toho University School of Medicine 5-21-16 Omorinishi Otaku, Tokyo, 143-8540, Japan.

Received: 30 March 2015.
First decision: 1 May 2015.
Accepted: 10 June 2015.

eISSN: 1529-7268 http://www.biolreprod.org
ISSN: 0006-3363

MATERIALS AND METHODS

Mouse Oocyte/Egg/Embryo Collection, Cell Culture, and Microinjection

Full-grown, germinal vesicle (GV)-intact oocytes, MII eggs, fertilized eggs, and preimplantation embryos were collected as previously described [20, 21]. GV oocytes were cultured in Chatot-Ziomek-Brinster (CZB) medium, which contains 5 mg/ml bovine serum albumin [22] and 2.5 μM milrinone (Sigma, St. Louis, MO) to inhibit GV breakdown (GVBD) [23]; MII eggs were cultured in CZB medium and fertilized eggs/embryos cultured in KSOM [24]. MI eggs were collected 6 h after transferring oocytes to milrinone-free CZB medium. All the animal experiments were approved by the Institutional Animal Use and Care Committee and were consistent with National Institutes of Health (NIH) guidelines.

GV oocytes were microinjected with approximately 5 pl of cRNA (0.5 μg/μl) or small interference (siRNA) (100 μM) in bicarbonate-free Whitten medium supplemented with 10 mM Hepes, 0.01% polyvinyl alcohol, and 2.5 μM milrinone as previously described [25]. Following microinjection, oocytes were returned to CZB medium with 2.5 μM milrinone or transferred to milrinone-free medium to permit resumption of meiosis. In vitro matured MII eggs were activated by incubating them in CZB medium containing 5 mM $SrCl_2$, 2 mM ethylene glycol tetraacetic acid, and 5 μg/ml cytochalasin D for 6 h [26]. Following activation, the cells were cultured at 37°C in an air atmosphere containing 5% CO_2.

Immunoblotting and Immunocytochemistry

Equal numbers (50–200) of GV oocytes, MI eggs, MII eggs, fertilized eggs, and embryos were lysed in 2× SDS loading buffer (Sigma), run on a 10% SDS-PAGE, and transferred to a PVDF membrane (Amersham, Piscataway, NJ). The following antibodies/antisera were used for Western blot analysis: mouse monoclonal anti-CNOT7 antibody (Sigma-Aldrich) at 1:3000 dilutions and rabbit anti-PAN2 antibody (ProteinTech Group, Chicago, IL) at 1:2000 dilutions. Immunodetection was performed using horseradish peroxidase-conjugated secondary antibodies and ECL prime reagents (Amersham) according to the manufacturer's instructions. As a loading control, membranes were stripped and reprobed with a mouse anti-TUBB antibody (Sigma) at 1:20 000 dilution.

For immunocytochemistry, oocyte, egg or embryo samples were fixed in 2.5% paraformaldehyde for 40 min at room temperature. The cells were then permeabilized for 15 min in PBS containing 0.2% Triton X-100, blocked in PBS containing 0.2% immunoglobulin G-free bovine serum albumin and 0.01% Tween-20 for 30 min (blocking solution) and then incubated with the primary antibody for 1 h at room temperature. RNA pol II C-terminal domain (CTD) phospho-ser2 antibody (Active Motif, Carlsbad, CA) was used at 1:200 dilution. After four 15 min washings in blocking medium, samples were incubated for 1 h with appropriate cy5-conjugated secondary antibody (Jackson ImmunoResearch, West Grove, PA) diluted 1:100 in blocking solution. After an additional three 15-min washings in blocking solution, the samples were mounted in Vectashield mounting solution containing Sytox green (Vector Laboratories, Burlingame, CA). Images were captured by a Leica TCS SP laser-scanning confocal microscope.

DNA Constructs and Mutagenesis

To generate luciferase reporters with a *Cnot7, Pan2,* or *Cnot6l* 3′ untranslated region (UTR), a short version of 3′ end of the UTR for each gene was amplified from mouse oocyte cDNA using the following primers (forward primers are listed first and reverse primers are listed second throughout). For *Cnot7* 3′ UTR, 5′-TACTCTAGATTGGTTCTGGCTCATCC TATGTA-3′ and 5′-CGTGAATTCAGTAAGGGTAAAAGTGATGGA-3′ were used. For *Cnot6l* 3′ UTR, 5′-TCGATCTAGATGGCCATCATAT GCTTTTA-3′ and 5′-TCGAGAATTCACATAATGGAAAATTTCTTGT-3′ were used. The final 100 bp of the *Pan2* 3′ UTR was generated by oligonucleotides annealing and primer extension with the following oligonucleotides, 5′-TACTCTAGATTCTATCTCGAGTTTTGTTTTATTTTTT AAAAATTTTGCTTAAAACAGCATG-3′ and 5′-CGTGAATTCAATGAG ATAAAAATACTTTTATTTTATAAAACATGCTGTTTTAAGCAAAATT-3.′ The obtained 3′ UTRs were double digested by XbaI and EcoRI and inserted downstream of pIVT-luc reporter vector [19].

To generate luciferase reporters with a *Cnot7, Cnot6l,* or *Pan2,* the 3′ UTR with mutated cytoplasmic polyadenylation elements (CPEs) and the desired mutated sequences were introduced by using the QuikChange Lightning Multi Site-Directed Mutagenesis (Stratagene, Santa Clara, CA) according to the manufacturer's instruction as described below.

The following oligonucleotides were used to construct pIVT/*Cnot7* 3′ UTR variants: 5′-GCATTTATGAAATCACATTTATTTTGTATTTTTCTTGATA TAAAATGTACCTTAAGACTTGTTATCT-3′ was used to generate pIVT/*Cnot7* 3′ UTR/mutated HEX1 (AAUAAA to AAGAAA mutation) and followed by using 5′-GTGAATTCACCAAATCTCTCCATTATTTC TTTTTGTAGCATTTATGAAATCACATTT-3′ to generate pIVT/*Cnot7* 3′ UTR/mutated HEX1 and HEX2 (AAUAAA to AAGAAA mutation for both poly [A] signal). 5′-AACAAATCAAGAACATCATAAATATGTTTA TAACCTCAAACAGTAAGGGTAAAAGTGATGGAGTAAAAGG-3′ was used to generate pIVT/*Cnot7* 3′ UTR/mutated CPE1 (UUUUAUU to UUUGAGG mutation); 5′-GCATGTGTGTAACTCGTATACAATCCAAAT AAGAAGACTATTTCCTGTCATGACTGCTT-3′ was used to generate pIVT/*Cnot7* 3′ UTR/mutated CPE2 (UUUUUAU to UUUGGAU mutation); 5′-AACAAATCAAGAACATCATAAATATGTTTATAACCTCAAACAGTAA GGGTAAAAGTGATGGAGTAAAAGG-3′ and 5′-GCATGTGTGTAA CTCGTATACAATCCAAATAAGAAGACTATTTCCTGTCATGACTGCT T-3′ were used to generate pIVT/*Cnot7* 3′ UTR/mutated CPE1+2.

The following oligonucleotides were used to construct pIVT/*Pan2* 3′ UTR variants: 5′-CAGTGAATTCAATGAGATAAAAATACTTTTCTTTTATAA AACATGCTGTTTTAAGCAAAATTTTTAAAAAA-3′ was used to generate pIVT/*Pan2* 3′ UTR/mutated HEX (AAUAAA to AAGAAA mutation); 5′-TTTTATAAAACATGCTGTTTTAAGCAAAATTTTTAACCAATCCAACA AAACTCGAGATAGAATCTAGAATTACACGGCG-3′ was used to generate pIVT/*Pan2* 3′ UTR/mutated CPE1 (UUUUAUUUUUU to UUGGAUUGGUU mutation); 5′-CGACGGCCAGTGAATTCAATGAGATACCAATACTTTT ATTTTATAAAACATGCTGTTTTAA-3′ was used to generate pIVT/*Pan2* 3′ UTR/mutated CPE2 (UUUUUAU to UUGGUAU mutation); 5′-TTTTAT AAAACATGCTGTTTTAAGCAAAATTTTTAACCAATCCAACAAAACTC CGAGATAGAATCTAGAATTACACGGCG-3′ and 5′-CGACGGCCAGTGA ATTCAATGAGATACCAATACTTTTATTTTATAAAACATGCTGTTTTA A-3′ were used to generate pIVT/*Pan2* 3′ UTR/mutated CPE1+2.

The following oligonucleotides were used to construct pIVT/*Cnot6l* 3′ UTR variants: 5′-ATTCACATAATGGAAAATTTCTTGTTTCTTAAAAAT ATCACATTTTGATACTAGAAACAGTAAAG-3′ was used to generate pIVT/*Cnot6l* 3′ UTR/mutated HEX (AAUAAA to AAGAAA mutation); 5′-TGAATTCACATAATGGAAAATTTCTTGTTTATTACCAATATCACATT TTGATACTAGAAACAGTAAAGTG-3′ was used to generate pIVT/*Cnot6l* 3′ UTR/mutated CPE1 (UUUUUAAU to UUGGUAAU mutation); 5′-GTCTAGATTTGAATTAAGCTACTGTTGGATTCCCAAAGTTTGATGCCT CTATAT-3′ was used to generate pIVT/*Cnot6l* 3′ UTR/mutated CPE2 (UUUUAUU to UUGGAUU mutation); 5′-CTAGATGGCCATCATATGCTT GGAATCTTCGTTGCCATACTGTC-3′ was used to generate pIVT/*Cnot6l* 3′ UTR/mutated CPE3 (UUUUAAU to UUGGAAU mutation); 5′-TGAATTCAC ATAATGGAAAATTTCTTGTTTATTACCAATATCACATTTTGATACTAG AAACAGTAAAGTG-3′, 5′-GTCTAGATTTGAATTAAGCTACTGTTGGA TTCCCAAAGTTTGATGCCTCTATAT-3′, and 5′-CTAGATGGCCATCATA TGCTTGGAATCTTCGTTGCCATACTGTC-3′ were used to generate pIVT/*Cnot6l* 3′ UTR/mutated CPE1+2+3.

To generate the *Cnot7* overexpression construct, mouse *Cnot7*-coding region was amplified from MGC mouse *Cnot7* cDNA (CloneId:3590764, Open Biosystems) using the following primers: 5′-ATCCTGCAGCCACCATGCC AGCAGCAACCGTAGATCA-3′ and 5′-GTCTCTAGACCTGTCATGAC TGCTTGCTG-3′. After Pst I and Xba I double digestion, the *Cnot7*-coding region was subcloned into pIVT vector for in vitro transcription.

To generate the Flag-*Cnot6l* overexpression construct, mouse *Cnot6L*-coding region was amplified from mouse ovarian cDNA using the following primers: 5′-AATGCGGCCGCAAAGGAAAAATATGATCCTCCAGA TCCTC-3′ and 5′-AATCTCTAGAGCTGTACTCCACTACCTCCG-3′. Amplified Cnot6l-coding region was double digested by Not I and Xba I and subcloned into pIVT-flag vector for in vitro transcription.

In Vitro Transcription

The pIVT-*luc*/*Cnot7*/*Cnot6l*/*Pan2* 3′ UTR variants were verified by sequencing and then linearized by EcoRI digestion. Capped mRNAs were made by in vitro transcription with T7 mScript mRNA production System (CellSCRIPT, Madison, WI) according to the manufacturer's instructions. Following in vitro transcription, template DNAs were digested by adding RNase-free DNase, and synthesized mRNA was purified by MEGAclear kit (Ambion, Grand Island, NY), precipitated, and redissolved in RNase-free water. A single mRNA band of the expected size was observed for each RNA sample on 1% formaldehyde denaturing gel.

For generating cRNA encoding *Cnot7* or *Flag-Cnot6l*, following in vitro transcription, the synthesized cRNA was polyadenylated by A-Plus Poly (A) Polymerase (CellSCRIPT). Synthesized RNA was aliquoted and stored at −80°C.

Luciferase Reporter Assay

Full-grown GV oocytes were microinjected with 5 pl of pIVT-*luc* mRNA with *Cnot7*/*Cnot6l*/*Pan2* 3′ UTR variants (0.05 μg/μl). Injected oocytes were transferred to milrinone-free medium and matured in vitro for 18 h. Controls were injected GV oocytes cultured for 18 h in CZB containing 2.5 μM milrinone. Luciferase activity was assayed by lysing oocytes/eggs in 1× passive lysis buffer and analyzed using a dual-luciferase reporter assay system (Promega, Madison, WI) according to the manufacturer's instructions.

Small Interfering RNA-Mediated Knockdown of Cnot7

Full-grown GV oocytes were injected with *Cnot7* siRNA (On-TARGET-plus SMARTpool L-059073-05; Dharmacon, Lafayette, CO) as described above. Microinjected oocytes were cultured in CZB with 2.5 μM milrinone for 20 h and then transferred to milrinone-free medium and allowed to mature to MII for 18 h. Total RNA was extracted from 30 eggs using a Pico-Pure RNA Isolation Kit (Applied Biosystems, Grand Island, NY) and used for quantitative PCR (qPCR) analysis or poly (A) tail length (PAT) assay.

PAT Assay

The PAT assay was carried out using a modified version termed rapid amplification of cDNA ends-PAT (RACE-PAT) [27]. Briefly, an ARCTURUS PicoPure RNA Isolation Kit (Applied Biosystems) was used to isolate total RNA. Oligo (dT)-based 3′ RACE primer (5′-AAGCAGTGGTAACAACG CAGAGTACGA $[t]_{12}$-3′) was used for reverse transcription by Superscript II reverse transcriptase (Invitrogen, Grand Island, NY) following the manufacturer's instruction. PCR-based PAT assay were carried out using 3′ RACE primer 5′-AAGCAGTGGTAACAACGCAGAGT-3′ and one of the following gene-specific primers for PAT assay: *Cpsf4l*, 5′-AGGGAGGAGTCATTCAT GAGCC-3′; *Gtsf1*, 5′-CCAGTTTCTGTGGCAACAACAG-3′; *Foxj3*, 5′-TGGTGACATGCATTGGCTTTTG-3′; *Bud3l*, 5′-GTCGCATCATCGAGTG CACACA-3′; *Tuba4a*, 5′-ATTCTTCTTGCTGCTGCTTCAC-3′; *Elp2*, 5′-TTGACTGCACCCTCCCCATCTT-3′; *Zp2*, 5′-GAAGACACAATGACGGT TAGCC-3′; *Zp3*, 5′-CGCCAGTGGTCCAAGCTAGTTT-3′; *Ppil3*, 5′-AAGC AGCCACACTTGGACAT-3′. Detailed PAT assay conditions for each transcript are available upon request. Amplicons were labeled by adding 1 μl $[P^{32}]$-α-ATP (0.001 mCi) per PCR reaction, and the reaction products were separated on 5% DNA polyacrylamide gel. After fixation in 7% acetic acid and vacuum dried to blotting paper, the gel was exposed to Phosphor image system overnight and scanned on Typhoon 9410 Scanner (GE Healthcare Life Sciences, Pittsburgh, PA). Acquired images were processed by Image J (NIH). As input control, an aliquot of extracted total RNA was reverse transcribed using random primers, and the coding region of the housekeeping gene *Actb* (5′-tccctgtatgcctctggtcg-3′ and 5′-cgtcaggcagctcatagctc-3′) was amplified to verify that RNA input for each PAT assay was similar.

Oligo(dT) Slot Blot

Oligo (dT) slot-blot analysis was performed as previously described with some minor modifications [28]. Briefly, total RNA extracted from mouse oocytes/eggs was transferred to a nitrocellulose membrane using a slot-blot apparatus (Schleicher and Schuell Minifold, Keene, NH). After air drying for 2 h at room temperature and ultraviolet crosslinking using a Stratagene UV Stratalinker 1800, the membranes were then hybridized with radiolabeled oligo $(dT)_{20}$ (Invitrogen) in ULTRAhyb Ultrasensitive Hybridization Buffer (Ambion) at 30°C overnight. The membranes were next washed twice by 2× SSC with 0.5% SDS for 5 min at 30°C, then exposed to the Phosphor image system overnight and scanned using a Typhoon 9410 Scanner (GE Healthcare Life Sciences). Acquired images were then processed by Image J (NIH). Each treatment was prepared in triplicate, and the experiment was performed three times.

RNA Isolation and Quantitative Real-Time PCR

Total RNA was isolated from 20–50 oocytes/eggs/embryos using a Picopure RNA Isolation kit (Applied Biosystems) and reverse transcribed by Superscript II reverse transcriptase (Invitrogen) using random hexamers as primers. The resulting cDNA was quantified by real-time PCR using an ABI Prism 7000 thermocycler (Applied Biosystems). The ABI TaqMan Assay-on-Demand probe/primer sets used were Mm00516123_m1 for *Cnot7*; Mm00659843_m1 for *Pan2*; Mm00523339_m1 for *Cnot6l*; Mm00518337_m1 for *Cpsf4l*; Mm01298413_m1 for *Gtsf1*; Mm00554610_m1 for *Foxj3*; Mm01200170_mH for *Bud31*; Mm00849767_s1 for *Tuba4a*; Mm00491325_m1 for *Elp2*; Mm00442173_m1 for *Zp2*; and Mm00442176_m1 for *Zp3*. PCR conditions were 40 cycles of 95°C for 15 sec and 60°C for 60 sec. Each sample was analyzed in triplicates. Quantification was normalized to the spiked exogenous *Gfp* mRNA using the comparative Ct method (ABI Prism 7700 Sequence Detection System; Applied Biosystems).

Global Transcription Assay

Global transcription was measured using a Click-iT RNA Imaging Kit (Invitrogen) according to the manufacturer's instructions. Briefly, 2-cell parthogenotes (generated as described under *Mouse Oocyte/Egg/Embryo Collection, Cell Culture, and Microinjection*) were cultured with 2 μM 5-ethynyl uridine (EU) in CZB medium for 1 h before fixation in 3.7% paraformaldehyde for 1 h at room temperature. After washing and permeabilization, incorporated EU was detected and visualized by confocal microscopy.

Statistical Analysis

One-way ANOVA were used to evaluate the differences between groups using Microsoft Excel software. A level of $P < 0.05$ was considered to be significant.

RESULTS

Cnot7, Pan2, and Cnot6l Are Dormant Maternal mRNAs That Are Mobilized During Oocyte Maturation

Dormant maternal mRNAs are a class of mRNAs in oocytes that are either not translated (or poorly translated) in the oocyte but whose translation markedly increases during maturation and results in a significant increase in the amount of protein. Accordingly, we conducted immunoblotting analyses on the well-conserved deadenylases PAN2 (and its regulatory subunit PAN3), CNOT6, and CNOT7 to ascertain whether their abundance increased during maturation. CNOT6L was not included in this analysis because we could not find an antibody that was suitable for immunoblotting or immunocytochemistry. Both CNOT7 and PAN2 increased during maturation whereas there was only a small increase CNOT6 (Fig. 1A). The increase in CNOT7 and PAN2 occurred between MI and MII (Fig. 1B). The relative abundance of CNOT7 remained elevated in the 1- and 2-cell stages but then exhibited a modest decline, whereas CNOT6 remained essentially constant during preimplantation development. The amount of PAN2 displayed a marked decreased between the 2-cell and blastocyst stages. The relative abundance of PAN3 was fairly constant, and the electrophoretic mobility shift detected between the GV and MII stages likely reflects loss of a posttranslational modification, which could be phosphorylation [29].

Another hallmark of dormant maternal mRNAs is the presence of a CPE in the 3′ UTR [30, 31]. In silico analysis revealed the presence of putative CPEs in the 3′ UTRs of *Cnot7*, *Cnot6l,* and *Pan2* transcripts (Fig. 2). Even though we could not detect CNOT6L by immunoblotting or immunocytochemistry, we focused our attention on *Cnot6l* rather than *Cnot6* because our microarray data indicated that *Cnot6l* transcripts are far more abundant than *Cnot6* transcripts in oocytes with raw scores of 1700 and 150, respectively. Note that CNOT6 and CNOT6L are incorporated into the CCR4/NOT complex in a mutually exclusive fashion [32]. To confirm that these CPEs can recruit dormant *Cnot7, Cnot6l,* and *Pan2* mRNAs for translation during oocyte maturation, we generated *Luc* reporter cRNAs in which the *Renilla luciferase* coding sequence was fused downstream with a short version of 3′ UTR of *Cnot7, Cnot6l,* and *Pan2*, respectively.

Reporter mRNAs were injected into the cytoplasm of GV oocytes, and a portion of injected oocytes were allowed to mature in vitro to MII eggs at which time luciferase activity was assayed; control oocytes were cultured for a similar length

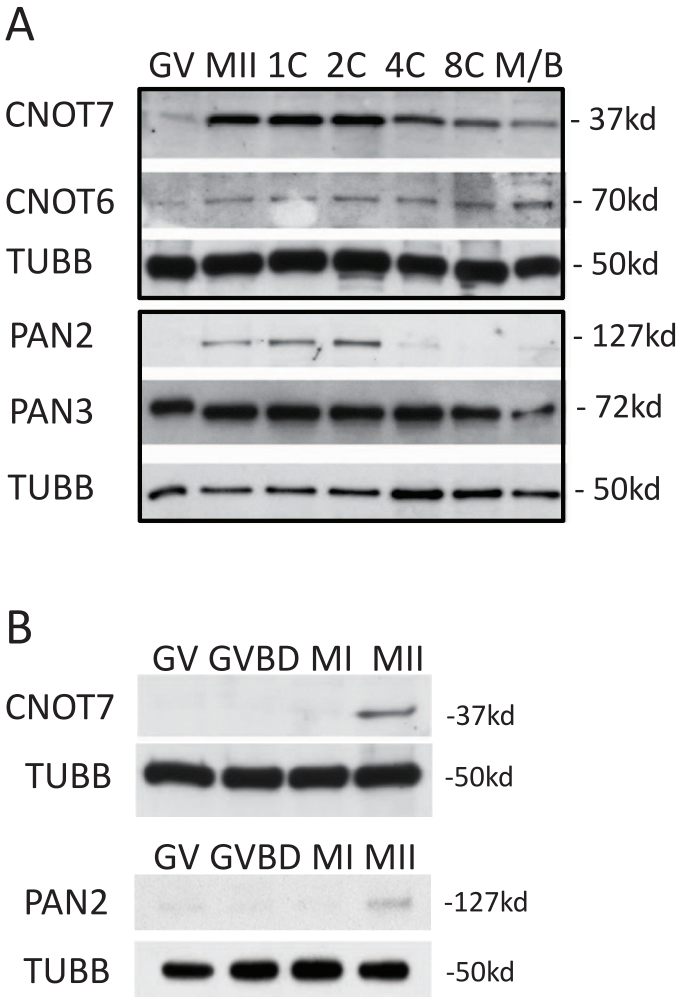

FIG. 1. Components of the 3′ RNA degradation machinery are encoded by dormant mRNAs recruited during oocyte maturation. **A**) Immunoblot analysis of deadenylation components CNOT6 and CNOT7 as well as PAN2 and PAN3 during oocyte maturation and early embryonic development. Two hundred oocytes/embryos were used for each stage. After probing with specific antibodies, the blots were stripped and reprobed with TUBB antibody as a loading control. The experiment was conducted two times, and similar results were obtained. GV, germinal vesicle-stage oocyte; MII, meiosis II egg; 1C, 1-cell embryo; 2C, 2-cell embryo; 4C, 4-cell embryo; 8C, 8-cell embryo; M/B, morula and blastocyst-stage embryo. **B**) CNOT7 and PAN2 expression during oocyte maturation. GV, germinal vesicle stage; GVBD, germinal vesicle breakdown; MI, metaphase I; MII, metaphase II. Two hundred oocytes/eggs per sample were used. The experiment was conducted two times, and similar results were obtained. The blot was stripped and reprobed with TUBB antibody as a loading control.

of time in milrinone-containing medium to maintain GV arrest. As anticipated, the 3′ UTR containing the putative CPEs stimulated translation as assessed by the increase in luciferase activity in MII eggs relative to that in GV oocytes (Fig. 2A).

We next identified the CPEs responsible for stimulating translation using a mutagenesis strategy. For *Cnot7*, there are two putative CPEs, which are 811 bp apart, and two consecutive polyadenylation hexanucleotide (HEX) AAUAAA sequence. Mutating either CPE1 or CPE2 or both significantly reduced *Cnot7* reporter activity (Fig. 2B). These results suggest both CPE1 and CPE2 are essential for recruitment of *Cnot7* into translation during oocyte maturation. In addition, mutating the cluster of two consecutive HEX AAUAAA substantially reduced luciferase activity, which is consistent with a previous report that both HEX and CPEs are required for cytoplasmic polyadenylation [31]. *Cnot6l* has three putative CPEs in the proximity of the AAUAAA HEX. Mutation of any of them reduces *Cnot6l* reporter activity (Fig. 2C), which suggests that all three CPEs within *Cnot6l* 3′ UTR are involved in recruitment of *Cnot6l*. For *Pan2*, there are two CPEs clustered around HEX, and mutation of CPE1 or CPE2 partially reduced *Pan2* reporter activity, with the double-mutation of CPE1 and CPE2 further reducing luciferase activity to that comparable with mutation of HEX (Fig. 2D). These results suggest that both of the CPEs are required for mobilization of *Pan2* during meiotic maturation.

Knocking Down CNOT7 Dramatically Reduces Deadenylation of Selected Maternal mRNAs During Oocyte Maturation

As described above, we could not detect CNOT6L by immunoblotting or immunocytochemistry, which excluded pursuing functional studies using a siRNA approach because we would not be able to document our ability to inhibit the maturation-associated increase in CNOT6L protein. Although we could detect CNOT6 by immunoblotting, such experiments required 200 oocytes per sample, which effectively precluded analyzing CNOT6 function because these experiments would employ a microinjection approach. In addition, CNOT6 exhibited only a very modest increase in its amount during maturation. This fact, coupled with *Cnot6* mRNA being much less abundant than *Cnot6l* mRNA, made CNOT6 an unattractive candidate to pursue functional studies. Therefore, we focused our attention on the role of *Cnot7* mRNA recruitment during maturation.

The maturation-associated increase in CNOT7 was effectively inhibited using a siRNA approach (Fig. 3A), and we did not observe any effect on the incidence of maturation and polar body emission. To examine the effect of inhibiting this increase on degradation of the endogenous mRNAs, a panel of maternal transcripts was selected using results of two independent microarray experiments [8, 33]. The selected transcripts are abundant in oocytes, and their abundance is significantly reduced from the GV to MII stage. The PAT assay demonstrated that these transcripts were deadenylated during maturation (Fig. 3B). The average length of the poly (A) tail of the eight transcripts ranged from 50–100 nucleotides in GV oocytes and was substantially shortened following maturation to MII. When the maturation-associated increase in CNOT7 was inhibited, deadenylation was substantially attenuated such that on average the length of the poly (A) tail of the transcripts as determined by densitometry was 68% ± 6% their length in GV oocytes. In addition, the intensity of the signal was markedly increased, being on average 55% ± 3% that in GV oocytes. The difference in signal intensity was unlikely due to variation in sample loading because the *Actb* signal was similar when random primers were used for reverse transcription. As described further below, the reduction in PAT assay signal in MII eggs was most likely due to the inefficiency of the oligo (dT) priming due to the shortened poly (A) tail when compared to using RNA from GV oocytes.

Exogenous Expression of CNOT7 Shortens the Length of the Poly (A) Tail of Maternal mRNAs in GV Oocytes

We next examined whether expressing CNOT7 to levels comparable to those reached in MII eggs can promote deadenylation in GV-intact oocytes. To this end, the concentration of *Cnot7* cRNA was adjusted so that following injection

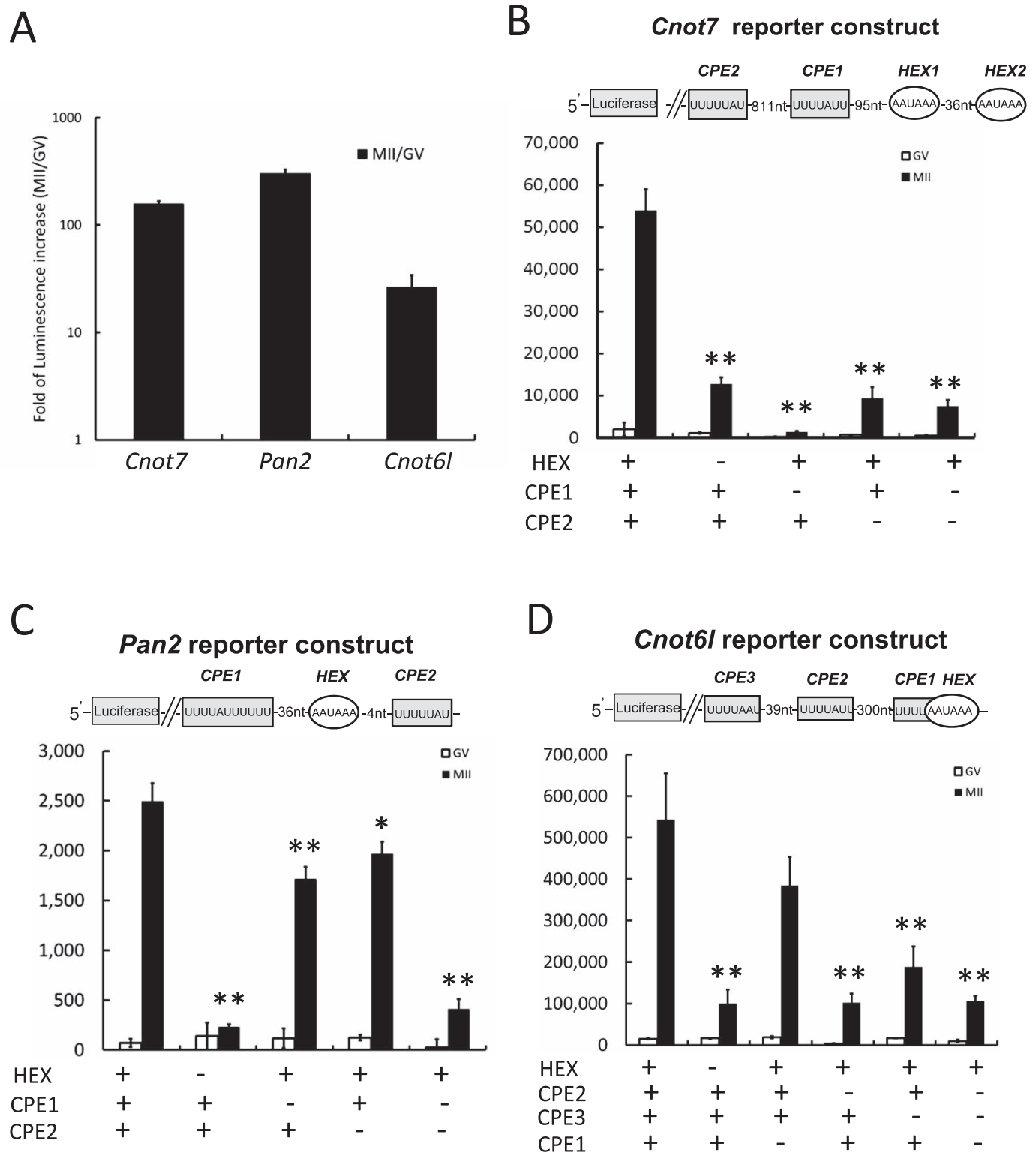

FIG. 2. The 3′ UTRs of *Cnot7, Pan2,* and *Cnot6l* promotes reporter mRNA translation during mouse oocyte maturation. **A**) Luciferase assay of reporter mRNAs containing *Cnot7, Cnot6l,* or *Pan2* 3′ UTR. *Luc* reporter cRNAs with a portion of *Cnot7, Cnot6l,* or *Pan2* 3′ UTR were injected into GV oocytes. Following maturation, luciferase activity was analyzed in individual eggs. Injected oocytes cultured in milrinone-containing medium to inhibit maturation served as the controls. The experiment was performed three times, and data are expressed as the mean ± SEM. **B**–**D**) *Luc* reporter cRNAs used to identify functional CPEs in *Cnot7, Cnot6l,* and *Pan2* 3′ UTRs. *Renilla* luciferase reporter activities were normalized to coinjected firefly luciferase control and are expressed as the mean ± SEM. The experiment was conducted three times. Statistically significant differences from controls are shown by asterisks (*$P <$ 0.05 and **$P < 0.01$).

into GV oocytes arrested from resuming maturation with milrinone the amount of CNOT7, as determined by immunoblotting following culture, was similar to that in oocytes matured to MII (Fig. 4A). As anticipated, the transcripts that were assayed all exhibited some degree of deadenylation (Fig. 4B) as well as a reduced signal intensity, which again likely

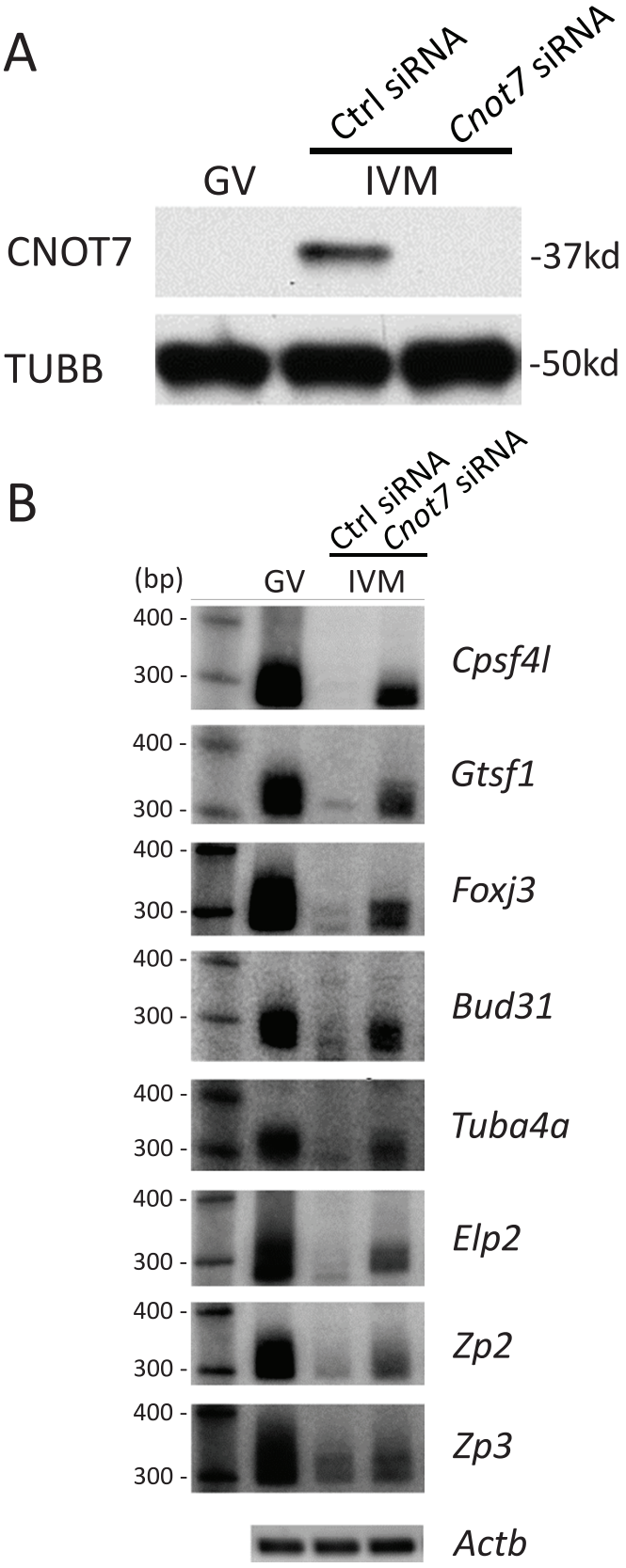

FIG. 3. Effect of *Cnot7* knockdown on maternal mRNA deadenylation during oocyte maturation. **A**) The effect of siRNA on inhibiting the maturation associated increase of CNOT7 as assayed by immunoblotting. GV, control uninjected oocytes; IVM, in vitro matured MII eggs. Oocytes injected with scrambled siRNA control or with *Cnot7* targeting siRNAs and matured to MII. After probing with CNOT7 antibody, the blot was stripped and reprobed with TUBB antibody as a loading control. Fifty oocytes per sample were used. The experiment was repeated three times, and similar results obtained; shown is a representative immunoblot. **B**) PAT analysis of selected maternal transcripts in *Cnot7*-knockdown MII oocytes. Oocytes were injected with either scrambled siRNA control or *Cnot7* targeting siRNAs. Total RNA was extracted and used for the PAT assay based on 3′ RACE-PAT. An aliquot of extracted total RNA was reverse transcribed using random primer, and *Actb* was amplified to verify that RNA input for each PAT assay is similar. The experiment was repeated three times, and similar results obtained; shown is a representative gel. Note that the gene-specific primers are located 250–300 nucleotides from where polyadenylation commences.

reflected reduced efficiency of oligo (dT) priming. On average, the length of the poly (A) tail of the transcripts and signal intensity in the CNOT7-expressing oocytes as determined by densitometry was 53% ± 6% and 47% ± 3%, respectively, that in GV-intact oocytes. As before, the difference in signal intensity was unlikely due to variation in sample loading because the *Actb* signal was similar when random primers were used for reverse transcription.

Altering CNOT7 Expression Levels Changes the Total Amount of Poly (A)-Containing RNA

The results described above using a limited number of transcripts suggest a role for CNOT7 in deadenylation of mRNAs that occurs during maturation. To extend these finding to the entire pool of poly (A)-containing RNAs, we analyzed the effect of inhibiting the maturation-associated increase in CNOT7 or expressing CNOT7 in GV-intact oocytes on the total amount of poly (A) RNA. We first established assay conditions in which the amount of oligo (dT) hybridized was a linear function of the number of oocytes from which total RNA was isolated (Fig. 5A). We then examined the effect of experimentally manipulating the amount of CNOT7 in oocytes and eggs on the amount of poly (A) RNA. The results of these experiments documented a 50% decrease in the total amount of poly (A) RNA that occurs during maturation (Fig. 5B), which is consistent with previous results [34]. This decrease was not as pronounced when the maturation-associated increase in CNOT7 was inhibited and was partially induced when CNOT7 was expressed in GV-intact oocytes. These results strongly suggest that *Cnot7* mobilization during maturation regulates the deadenylation of maternal mRNAs at a global level.

Altering the Amount of CNOT7 Effects Adenylation but Does Not Result in Complete mRNA Degradation

As described above, in somatic cells deadenylation typically leads to rapid degradation of the targeted mRNA. Such, however, is unlikely the fate of many mRNAs during maturation; for example, quantitative RT-PCR (qRT-PCR) using random primers to generate cDNA reveals a range of mRNA degradation from ~30% to almost complete degradation (e.g., see [4]). As anticipated, the transcripts analyzed in this study displayed different degrees of degradation following maturation when transcript abundance was assayed by qRT-PCR using random primers and gene-specific probes (Fig. 6). Inhibiting the maturation-associated increase in CNOT7 had little, if any effect, on the degradation fate of the transcript (Fig. 6A), whereas there was a pronounced effect on the length of the poly (A) tail (Fig. 3). Likewise, expressing CNOT7 in GV-intact oocytes had little effect on inducing mRNA degradation (Fig. 6B) but did initiate deadenylation (Fig. 4). By the 2-cell

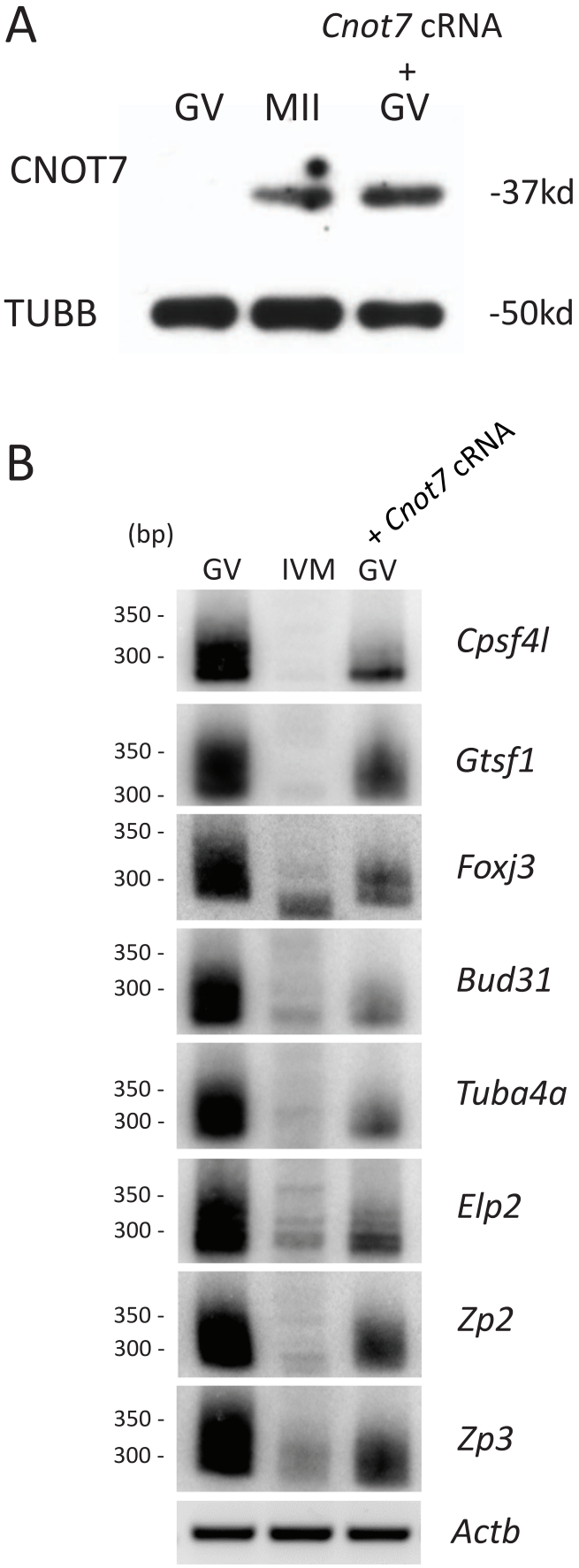

FIG. 4. Effect of *Cnot7* overexpression on the length of the poly(A) tail of maternal mRNAs in GV oocytes. **A**) The relative amount of expression of exogenous *Cnot7* was determined by immunoblotting, and the concentration of *Cnot7* cRNA was adjusted to generate an amount similar to the endogenous amount of CNOT7 following maturation. After probing with CNOT7 antibody, the blot was stripped and reprobed with TUBB antibody as loading control. **B**) PAT analysis of selected maternal transcripts in *Cnot7*-overexpressed GV oocytes. Oocytes injected with cRNA coding *Cnot7* were used for this assay. Total RNA were extracted and used for the PAT assay based on 3′ RACE-PAT. An aliquot of extracted total RNA was reverse transcribed using random primer, and *Actb* was amplified to verify that RNA input for each PAT assay is similar. The experiment was repeated three times, and similar results obtained; shown is a representative gel.

stage, these mRNAs were essentially totally degraded (Fig. 6C).

Inhibiting Deadenylation Inhibits Zygotic Genome Activation

We previously reported that inhibiting the maturation-associated increase in DCP1A and DCP2 reduced transcription in 2-cell embryos by 50% [19]. To ascertain whether a similar situation exists for CNOT7, we inhibited the maturation-associated increase in CNOT7, and following maturation, the MII eggs were activated by $SrCl_2$ treatment and diploidized by treatment with cytochalasin D [35]. Global transcription in the 2-cell embryos was then assessed by EU incorporation. Results of these experiments demonstrated that inhibiting the increase in CNOT7 reduced global transcription by ~70% (Fig. 7A). An ~50% decrease was observed when the embryos were stained with antibodies that specifically recognize CTD S2 phosphorylation, which is a marker for RNA polymerase II engaged in transcription (Fig. 7B).

DISCUSSION

We report here that recruitment of dormant maternal mRNA encoding CNOT7, a deadenylase, contributes to the transition from mRNA stability to instability initiated by resumption of meiosis of mouse oocytes. Taken with our previous work on MSY2 and DCP1A/DCP2 the picture that emerges is that mRNAs are stable in oocytes because the activity of the RNA degradation machinery is intrinsically low with mRNAs further protected from degradation by their association with MSY2. Maturation triggers recruitment of critical components involved in RNA degradation from both the 5′ and 3′ ends, with phosphorylation of MSY2 making mRNAs more susceptible to the degradation machinery. These changes initiate the oocyte-to-embryo transition, which entails transforming a highly differentiated oocyte into totipotent blastomeres and loss of oocyte identity. Initiation of mRNA degradation is also critical for subsequent developmental events to occur correctly, for example, genome activation. This finding is consistent with results obtained from other organisms demonstrating that deadenylation is essential for early embryonic development [16, 36–38]. It is interesting to note that in *Xenopus* oocytes, PARN (a cap-dependent deadenylase) is sequestered in the nucleus, and following nuclear membrane breakdown, it is released into the cytoplasm where it is involved in maternal mRNA degradation [16]. This alternative strategy of sequestering deadenylases would provide an additional safeguard to ensure maternal mRNA longevity. A role of PARN, if any, in degradation of maternal mRNAs in mouse oocytes is not known.

PAN2, the catalytic moiety of the PAN2-PAN3 deadenylase complex, is also encoded by a dormant maternal mRNA. Consistent with oocyte mRNAs possessing a short

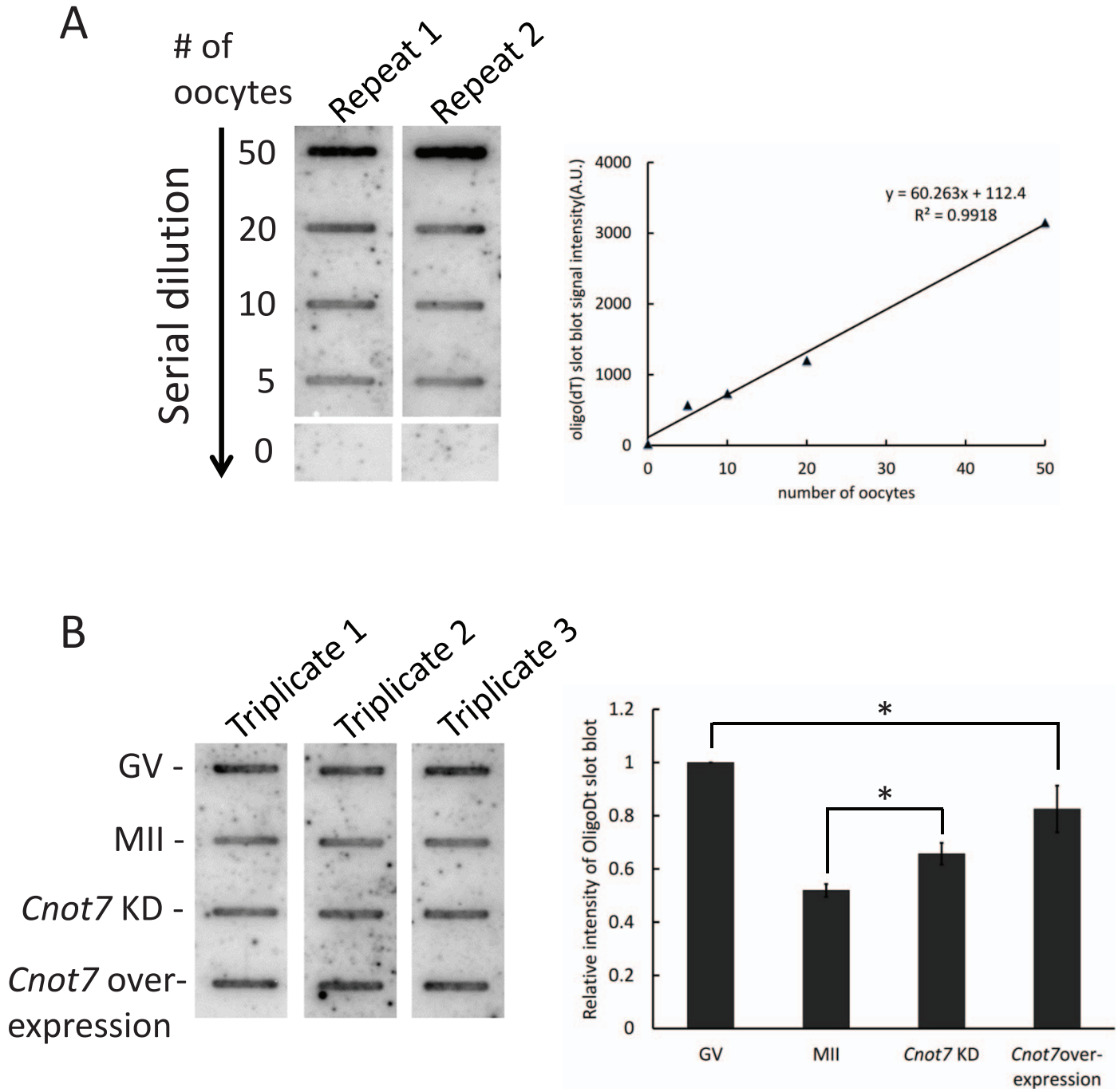

FIG. 5. Quantitative change of total amount of poly (A)-containing mRNA in *Cnot7*-knockdown MII eggs or when *Cnot7* is overexpressed in GV oocytes. **A**) Establishment of oligo (dT) slot blot calibration curve. Oocytes (0, 5, 10, 20, and 50) were used as input to establish a calibration curve. Each sample was spotted in duplicate, and each lane represents one of the duplicates. Signal intensity was captured using a Phosphor image system and quantified by Image J software. After subtraction of background, signal intensities from each paired duplicates were averaged and then plotted against number of oocyte input to establish calibration curve and regression analysis. Regression analysis of total amount determination of poly (A)-containing mRNA by oligo (dT) slot blot ($Y = 60.263x+112.4$; $r^2 = 0.9918$). The intercept was not significantly different from zero. **B**) Global change in total amount of poly (A) in *Cnot7*-knockdown MII eggs or oocytes expressing *Cnot7*. For each experiment, each sample was spotted in triplicate, and each lane represents one of the triplicates; shown are the results of one experiment. Twenty-five oocytes/egg were used for each sample, and the experiment was repeated three times. Signal intensity was captured by Phosphor image system and quantified by Image J software. The average value from the triplicate samples was used, and after subtraction of the background, signal intensities from the three experiments were averaged. The data are presented as mean ± SEM. Statistically significant differences are shown by asterisk (*$P < 0.05$).

poly (A) tail is that inhibiting the maturation-associated increase in PAN2 has little, if any, effect on deadenylation (Supplemental Fig. S1, available online at www.biolreprod.org); PAN does not totally degrade the poly (A) and leaves ~25 A residues [39]. Although the PAN2-PAN3 complex may not have a primary role in initiating mRNA degradation from the 3′ end, an increase in its activity via mobilization of *Pan2* mRNA during maturation provides a plausible expla-

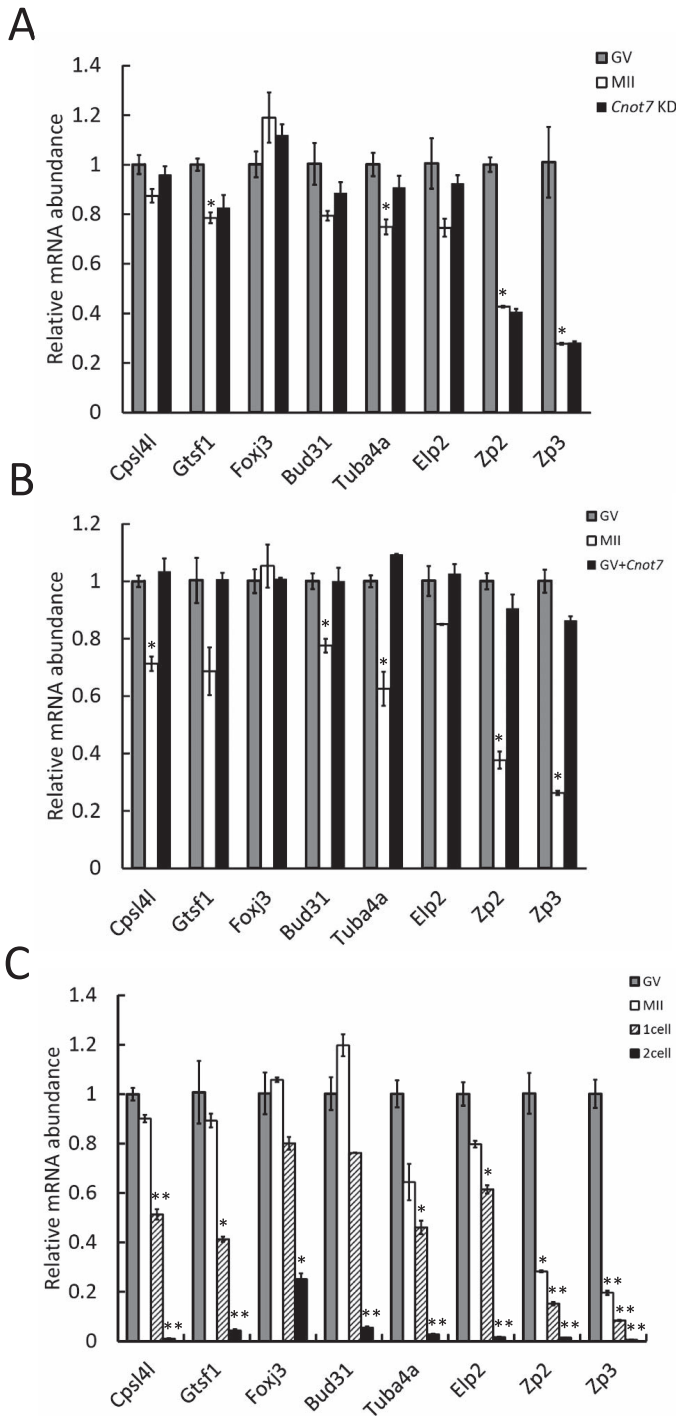

FIG. 6. Effect of *Cnot7* knockdown and ectopic expression on maternal mRNA stability. **A**) Quantitative PCR analysis of selected maternal transcripts to assess effect of *Cnot7* knockdown. GV oocytes were microinjected with siRNA targeting *Cnot7*, cultured for 20 h in milrinone-containing medium, and then transferred to milrinone-free medium to initiate maturation; MII eggs were then collected for qPCR analysis. Transcript abundance is expressed relative to that of scrambled siRNA-injected GV-intact oocytes. The experiment was performed three times, and data are expressed as the mean ± SEM. Gray bars, GV-intact oocytes; open bars, oocytes injected with scrambled siRNA and matured to MII; black bars, oocytes injected with siRNA targeting *Cnot7* and matured to MII. **B**) Quantitative PCR analysis of selected maternal transcripts in GV oocytes ectopically expressing *Cnot7*. GV oocytes were microinjected with *Cnot7* cRNA and then cultured for 20 h in milrinone-containing medium. Transcript abundance is expressed relative to that of noninjected GV-intact oocytes cultured in the same condition. The experiment was performed three times, and data are expressed as the mean ± SEM. Statistically significant differences from controls are shown by asterisk (*$P < 0.05$ and **$P < 0.01$). Gray bars, GV-intact oocytes; open bars, Noninjected oocyte in vitro matured (IVM) MII; black bars, oocytes injected with *Cnot7* cRNA. **C**) Messenger RNA degradation time course of selected maternal transcripts. GV, germinal vesicle-stage oocyte; MII, meiosis II egg; 1C, 1-cell embryo; 2C, 2-cell embryo. Relative abundance of selected maternal transcripts was determined by qPCR. Gray bars, GV oocyte; open bars, MII egg; diagonally stripped bars, fertilized 1-cell embryos; black bars, 2-cell embryos.

nation why female *Cnot7*$^{-/-}$ mice are fertile [40], that is, the PAN2-PAN3 complex would provide a compensatory function. We were not able to confirm this proposal because we were unable to inhibit the maturation-associated increase in both CNOT7 and PAN2.

Although we could not confirm by either immunoblotting or immunocytochemistry that a siRNA approach inhibited the maturation-associated increase in CNOT6L or whether we could express it to a level comparable with the endogenous amount of CNOT6L, we did note that siRNAs targeting *Cnot6l* mRNA partially reduced mRNA deadenylation (Supplemental Fig. S2) and that overexpressing CNOT6L in GV-arrested oocytes induced deadenylation (Supplemental Fig. S3). These effects, which were not as pronounced as for CNOT7, were anticipated because CNOT6L and CNOT7 reside in the same complex.

Recruitment of dormant maternal mRNAs encoding critical components of the RNA degradation machinery represents new members of this growing family that were previously serendipitously identified, for example, *Plat* [41]. Microarray data using oligo (dT) to generate cDNA [42] and analysis of mRNAs recruited to polysomes during maturation [7] has provided a means to identify on a global scale these maternal-recruited mRNAs and cis-acting 3′ UTR regulatory sequences that govern their recruitment. Analysis of these data reveals that dormant maternal mRNAs typically encode for proteins central to a process that should be minimal in the oocyte but then required by the 1-cell stage. For example, oocytes must not undergo a round of DNA replication between MI and MII, but need to replicate their DNA following fertilization. ORC6L, critical for assembly of a functional origin-of-replication complex, is encoded by a maternal-recruited mRNA, thereby ensuring that DNA replication does not occur between MI and MII but that the 1-cell embryo is capable of DNA synthesis [43]. Another feature of these mRNAs is that their relative abundance in oocytes is high but not at later stages of preimplantation development. Large amounts of these mRNAs likely enables the oocyte, which is a large cell, to synthesize and accumulate a sufficient amount of the protein in a short period of time before its function is required.

The results presented here also indicate that deadenylation often does not lead to total destruction of the targeted mRNA (*Zp2* and *Zp3* being exceptions), with partially degraded transcripts being stable until genome activation. This general conclusion was deduced more than 25 years ago by assessing changes in the amount of *actin* mRNA by Northern blot analysis and determining that the deadenylated mRNA is stable and only degraded following genome activation [34]. More recent studies using qRT-PCR and microarrays lead to the conclusion that such is the fate of many mRNAs (e.g., see [4]), as did a probe-level analysis of transcript abundance of microarray data [44]. This behavior, namely, partial degradation during maturation followed by terminal decay after genome activation, extends beyond mouse. For example, in

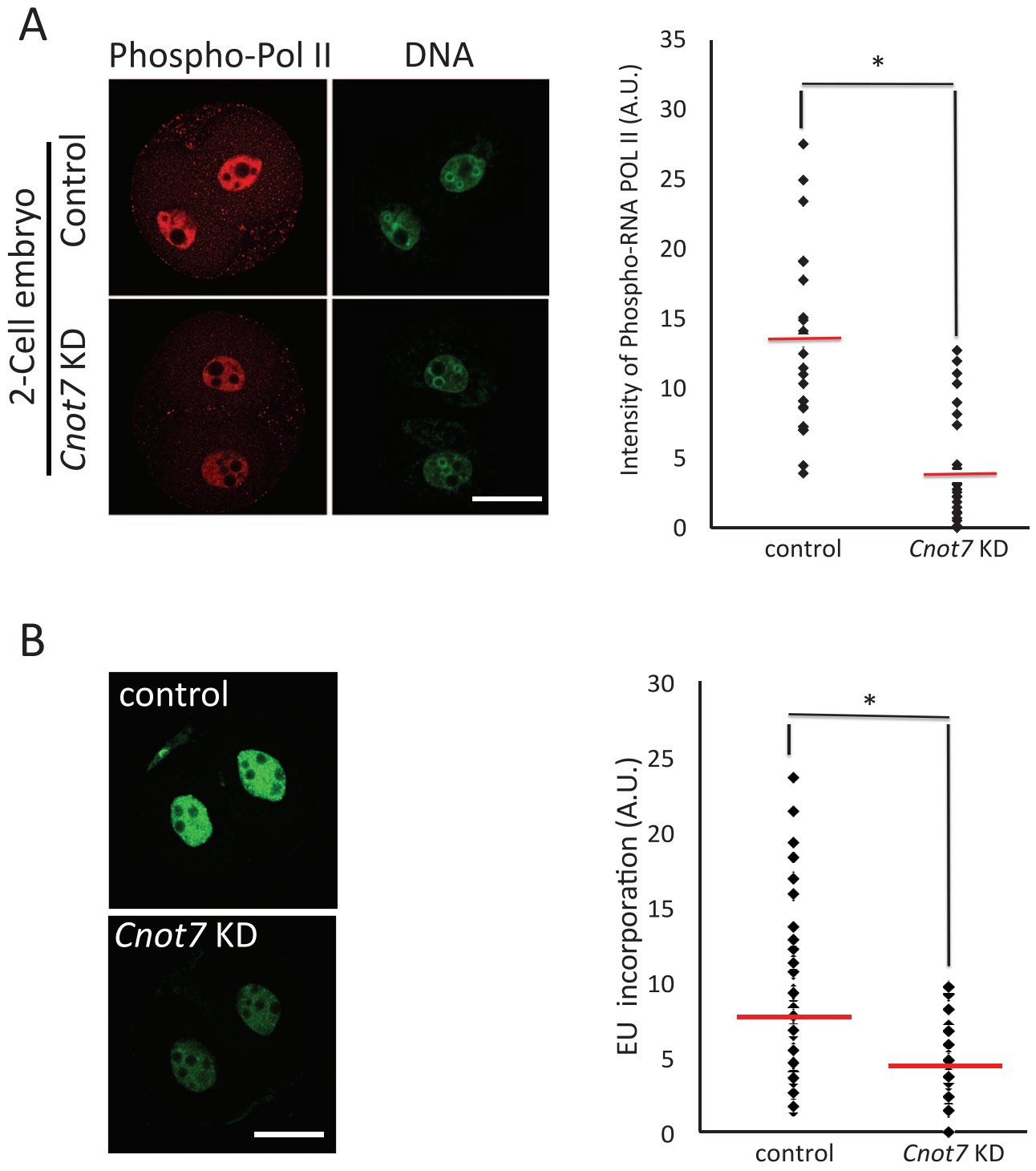

FIG. 7. Effect of inhibiting maturation-associated increase of CNOT7 on zygotic genome activation. **A**) Relative amount of phosphorylated CTD of RNA polymerase II is reduced following inhibition of maturation-associated increase of CNOT7 in activated 2-cell embryos. Representative staining images of control and *Cnot7*-knockdown 2-cell embryos by POLR2 CTD phosphor S2 antibody; quantification of the data are shown. The experiment was performed two times. The difference between the two groups is significant ($P < 0.05$). **B**) Global transcription in 2-cell embryos is reduced following inhibition of maturation-associated increase of CNOT7 by siRNA. Representative staining images of control and *Cnot7*-knockdown 2-cell embryos; quantification of the data are shown. The experiment was performed two times. The difference between the two groups is significant ($P < 0.05$). Bar = 25 μm.

Xenopus, deadenylation does not lead to mRNA destruction in oocytes, with mRNAs being degraded following genome activation [45–48].

Most intriguing is the finding that many deadenylated mRNAs are not degraded until the time of genome activation, which in mouse is ~2 days after initiation of maturation. The correlation between loss of MSY2 by the 2-cell stage and completion of degradation of maternal mRNAs could be causal, and studies using *Msy2*$^{-/-}$ oocytes could establish whether such a causal relationship exists. Last, resuming degradation of maternal mRNAs at the 2-cell stage could serve as a source of nucleotides to support transcription during

genome activation. This strategy would circumvent rapid catabolism of nucleotides if mRNAs were totally degraded during maturation and the poor ability of 1- and 2-cell embryos to transport ribonucleosides [49, 50]. Similar logic would apply to *Xenopus* in which development prior to genome activation occurs in a nutrient poor environment.

ACKNOWLEDGMENT

The authors thank Fabian L. Cardenas for conducting portions of the experiments shown in Figure 1.

REFERENCES

1. Brower PT, Gizang E, Boreen SM, Schultz RM. Biochemical studies of mammalian oogenesis: synthesis and stability of various classes of RNA during growth of the mouse oocyte in vitro. Dev Biol 1981; 86:373–383.
2. Jahn CL, Baran MM, Bachvarova R. Stability of RNA synthesized by the mouse oocyte during its major growth phase. J Exp Zool 1976; 197: 161–171.
3. Moore GP, Lintern-Moore S. Transcription of the mouse oocyte genome. Biol Reprod 1978; 18:865–870.
4. Medvedev S, Yang J, Hecht NB, Schultz RM. CDC2A (CDK1)-mediated phosphorylation of MSY2 triggers maternal mRNA degradation during mouse oocyte maturation. Dev Biol 2008; 321:205–215.
5. Yu J, Deng M, Medvedev S, Yang J, Hecht NB, Schultz RM. Transgenic RNAi-mediated reduction of MSY2 in mouse oocytes results in reduced fertility. Dev Biol 2004; 268:195–206.
6. Yu J, Hecht NB, Schultz RM. RNA-binding properties and translation repression in vitro by germ cell-specific MSY2 protein. Biol Reprod 2002; 67:1093–1098.
7. Chen J, Melton C, Suh N, Oh JS, Horner K, Xie F, Sette C, Blelloch R, Conti M. Genome-wide analysis of translation reveals a critical role for deleted in azoospermia-like (Dazl) at the oocyte-to-zygote transition. Genes Dev 2011; 25:755–766.
8. Su YQ, Sugiura K, Woo Y, Wigglesworth K, Kamdar S, Affourtit J, Eppig JJ. Selective degradation of transcripts during meiotic maturation of mouse oocytes. Dev Biol 2007; 302:104–117.
9. Wilusz CJ, Wormington M, Peltz SW. The cap-to-tail guide to mRNA turnover. Nat Rev Mol Cell Biol 2001; 2:237–246.
10. Garneau NL, Wilusz J, Wilusz CJ. The highways and byways of mRNA decay. Nat Rev Mol Cell Biol 2007; 8:113–126.
11. Goldstrohm AC, Wickens M. Multifunctional deadenylase complexes diversify mRNA control. Nat Rev Mol Cell Biol 2008; 9:337–344.
12. Yamashita A, Chang TC, Yamashita Y, Zhu W, Zhong Z, Chen CY, Shyu AB. Concerted action of poly(A) nucleases and decapping enzyme in mammalian mRNA turnover. Nat Struct Mol Biol 2005; 12:1054–1063.
13. Schaeffer D, van Hoof A. Different nuclease requirements for exosome-mediated degradation of normal and nonstop mRNAs. Proc Natl Acad Sci U S A 2011; 108:2366–2371.
14. Coller J, Parker R. Eukaryotic mRNA decapping. Annu Rev Biochem 2004; 73:861–890.
15. Liu H, Kiledjian M. Decapping the message: a beginning or an end. Biochem Soc Trans 2006; 34:35–38.
16. Korner CG, Wormington M, Muckenthaler M, Schneider S, Dehlin E, Wahle E. The deadenylating nuclease (DAN) is involved in poly(A) tail removal during the meiotic maturation of Xenopus oocytes. EMBO J 1998; 17:5427–5437.
17. Couttet P, Fromont-Racine M, Steel D, Pictet R, Grange T. Messenger RNA deadenylylation precedes decapping in mammalian cells. Proc Natl Acad Sci U S A 1997; 94:5628–5633.
18. Hu W, Sweet TJ, Chamnongpol S, Baker KE, Coller J. Co-translational mRNA decay in Saccharomyces cerevisiae. Nature 2009; 461:225–229.
19. Ma J, Flemr M, Strnad H, Svoboda P, Schultz RM. Maternally recruited DCP1A and DCP2 contribute to messenger RNA degradation during oocyte maturation and genome activation in mouse. Biol Reprod 2013; 88: 11.
20. Schultz RM, Montgomery RR, Belanoff JR. Regulation of mouse oocyte meiotic maturation: implication of a decrease in oocyte cAMP and protein dephosphorylation in commitment to resume meiosis. Dev Biol 1983; 97: 264–273.
21. Ma J, Svoboda P, Schultz RM, Stein P. Regulation of zygotic gene activation in the preimplantation mouse embryo: global activation and repression of gene expression. Biol Reprod 2001; 64:1713–1721.
22. Chatot CL, Ziomek CA, Bavister BD, Lewis JL, Torres I. An improved culture medium supports development of random-bred 1-cell mouse embryos in vitro. J Reprod Fertil 1989; 86:679–688.
23. Tsafriri A, Chun SY, Zhang R, Hsueh AJ, Conti M. Oocyte maturation involves compartmentalization and opposing changes of cAMP levels in follicular somatic and germ cells: studies using selective phosphodiesterase inhibitors. Dev Biol 1996; 178:393–402.
24. Erbach GT, Lawitts JA, Papaioannou VE, Biggers JD. Differential growth of the mouse preimplantation embryo in chemically defined media. Biol Reprod 1994; 50:1027–1033.
25. Kurasawa S, Schultz RM, Kopf GS. Egg-induced modifications of the zona pellucida of mouse eggs: effects of microinjected inositol 1,4,5-trisphosphate. Dev Biol 1989; 133:295–304.
26. Kishigami S, Wakayama T. Efficient strontium-induced activation of mouse oocytes in standard culture media by chelating calcium. J Reprod Dev 2007; 53:1207–1215.
27. Tremblay K, Vigneault C, McGraw S, Sirard MA. Expression of cyclin B1 messenger RNA isoforms and initiation of cytoplasmic polyadenylation in the bovine oocyte. Biol Reprod 2005; 72:1037–1044.
28. Mohanty BK, Giladi H, Maples VF, Kusher SR. Analysis of RNA polyadenylation in E. coli. In: Maquat L, Arraiano CM (eds.), Methods in Enzymology, RNA Turnover in Bacteria, Archaea and Organelles. San Diego, CA: Academic Press/Elsevier; 2008:3–29.
29. Huang KL, Chadee AB, Chen CY, Zhang Y, Shyu AB. Phosphorylation at intrinsically disordered regions of PAM2 motif-containing proteins modulates their interactions with PABPC1 and influences mRNA fate. RNA 2013; 19:295–305.
30. Mendez R, Richter JD. Translational control by CPEB: a means to the end. Nat Rev Mol Cell Biol 2001; 2:521–529.
31. Pique M, Lopez JM, Foissac S, Guigo R, Mendez R. A combinatorial code for CPE-mediated translational control. Cell 2008; 132:434–448.
32. Lau NC, Kolkman A, van Schaik FM, Mulder KW, Pijnappel WW, Heck AJ, Timmers HT. Human Ccr4-Not complexes contain variable deadenylase subunits. Biochem J 2009; 422:443–453.
33. Pan H, O'Brien MJ, Wigglesworth K, Eppig JJ, Schultz RM. Transcript profiling during mouse oocyte development and the effect of gonadotropin priming and development in vitro. Dev Biol 2005; 286:493–506.
34. Paynton BV, Rempel R, Bachvarova R. Changes in state of adenylation and time course of degradation of maternal mRNAs during oocyte maturation and early embryonic development in the mouse. Dev Biol 1988; 129:304–314.
35. Kubiak J, Paldi A, Weber M, Maro B. Genetically identical parthenogenetic mouse embryos produced by inhibition of the first meiotic cleavage with cytochalasin D. Development 1991; 111:763–769.
36. Molin L, Puisieux A. C. elegans homologue of the Caf1 gene, which encodes a subunit of the CCR4-NOT complex, is essential for embryonic and larval development and for meiotic progression. Gene 2005; 358: 73–81.
37. Morris JZ, Hong A, Lilly MA, Lehmann R. twin, a CCR4 homolog, regulates cyclin poly(A) tail length to permit Drosophila oogenesis. Development 2005; 132:1165–1174.
38. Reverdatto SV, Dutko JA, Chekanova JA, Hamilton DA, Belostotsky DA. mRNA deadenylation by PARN is essential for embryogenesis in higher plants. RNA 2004; 10:1200–1214.
39. Lowell JE, Rudner DZ, Sachs AB. 3′-UTR-dependent deadenylation by the yeast poly(A) nuclease. Genes Dev 1992; 6:2088–2099.
40. Nakamura T, Yao R, Ogawa T, Suzuki T, Ito C, Tsunekawa N, Inoue K, Ajima R, Miyasaka T, Yoshida Y, Ogura A, Toshimori K, et al. Oligo-astheno-teratozoospermia in mice lacking Cnot7, a regulator of retinoid X receptor beta. Nat Genet 2004; 36:528–533.
41. Huarte J, Belin D, Vassalli A, Strickland S, Vassalli JD. Meiotic maturation of mouse oocytes triggers the translation and polyadenylation of dormant tissue-type plasminogen activator mRNA. Genes Dev 1987; 1: 1201–1211.
42. Zeng F, Baldwin DA, Schultz RM. Transcript profiling during preimplantation mouse development. Dev Biol 2004; 272:483–496.
43. Murai S, Stein P, Buffone MG, Yamashita S, Schultz RM. Recruitment of Orc6l, a dormant maternal mRNA in mouse oocytes, is essential for DNA replication in 1-cell embryos. Dev Biol 2010; 341:205–212.
44. Salisbury J, Hutchison KW, Wigglesworth K, Eppig JJ, Graber JH. Probe-level analysis of expression microarrays characterizes isoform-specific degradation during mouse oocyte maturation. PLoS One 2009; 4:e7479.
45. Audic Y, Omilli F, Osborne HB. Postfertilization deadenylation of mRNAs in Xenopus laevis embryos is sufficient to cause their degradation at the blastula stage. Mol Cell Biol 1997; 17:209–218.
46. Graindorge A, Thuret R, Pollet N, Osborne HB, Audic Y. Identification of

post-transcriptionally regulated Xenopus tropicalis maternal mRNAs by microarray. Nucleic Acids Res 2006; 34:986–995.

47. Tafuri SR, Wolffe AP. Selective recruitment of masked maternal mRNA from messenger ribonucleoprotein particles containing FRGY2 (mRNP4). J Biol Chem 1993; 268:24255–24261.
48. Voeltz GK, Steitz JA. AUUUA sequences direct mRNA deadenylation uncoupled from decay during Xenopus early development. Mol Cell Biol 1998; 18:7537–7545.
49. Daentl DL, Epstein CJ. Developmental interrelationships of uridine uptake. Nucleotide formation and incorporation into RNA by early mammalian embryos. Dev Biol 1971; 24:428–442.
50. Epstein CJ, Daentl DL, Smith SA, Kwok LW. Guanine metabolism in preimplantation mouse embryo. Biol Reprod 1971; 5:308–313.